ELSEVIER

Polymer 40 (1999) 1547–1552

polymer

Effect of hydrogenation on dynamic mechanical relaxation: 2. Syndiotactic polystyrene

Hisayuki Nakatani[a], Koh-hei Nitta[a,*], Kazuo Soga[b]

[a]*Centre for New Materials, Japan Advanced Institute of Science and Technology, 1-1 Asahidai, Tatsunokuchi, Ishikawa 923-12, Japan*
[b]*School of Materials Science, Japan Advanced Institute of Science and Technology, 1-1 Asahidai, Tatsunokuchi, Ishikawa 923-12, Japan*

Received 19 December 1997; revised 10 April 1998; accepted 7 May 1998

Abstract

The dynamic mechanical behaviour of a series of hydrogenated syndiotactic polystyrenes (HsPS) with various degrees of hydrogenation has been investigated. In the case of crystallized HsPS samples, the primary dispersion is much broader due to the overlapping of two glass relaxation processes arising from one purely amorphous component and the other amorphous component under restraint by crystallites, as seen in semicrystalline polymers. There exist two secondary dispersions ascribed to chair–chair flip motion and oscillatory rotation of the cyclohexyl group in the range from 110 to 250 K. As compared with glassy complete HsPS, the strength of loss tangent (tan δ) peaks ascribed to the molecular motions of the cyclohexyl group in the crystalline polymer was lowered, suggesting that the molecular motions of this group in the crystalline part are sterically hindered.

Keywords: Dynamic mechanical properties; Hydrogenation; Syndiotactic polystyrene

1. Introduction

The hydrogenation technique is a powerful tool for the preparation of model materials with controlled microstructures for use in fundamental polymer studies [1–7]. Since this technique is capable of adding hydrogen to the unsaturated double bond while keeping up the molecular weight, molar mass distribution and stereochemistry of the original polymer, the hydrogenated polymer has been instrumental in investigating the effect of microstructures on various properties. From such a viewpoint, several types of polyolefins have been prepared so far using hydrogenation techniques. Hydrogenated atactic polystyrene (HaPS) shows a higher glass transition temperature [5,6], a lower density [7] and complex secondary relaxation processes [8] as compared with atactic polystyrene. Therefore, much attention has been paid to HaPS as a new glassy polyolefin with a high heat resistance.

Syndiotactic polystyrene (sPS) [9–11] is found to be a crystalline polymer with a high melting temperature of 543 K. Hydrogenated sPS (HsPS) is suggested to be also crystallizable because the aromatic rings are converted to cyclohexyl rings while keeping the stereochemistry [12]. Therefore, the HsPS has potential utility as a new crystalline polyolefin. In this work, we have investigated the dynamic mechanical properties and melting behaviour of a series of hydrogenated sPS with various degrees of hydrogenation, with the aim of clarifying the influence of microstructure units on mechanical relaxation behaviour in crystalline and amorphous phases as well as on local molecular motion in the semicrystalline state. The results thus obtained are also able to give a physical insight into the molecular motions responsible for the mechanical properties and visoelasticity of the crystalline copolymer.

2. Experimental

2.1. Materials

Styrene was commercially obtained from Nacalai Tesque Co. The styrene was washed with an aqueous solution of sodium hydroxide, dried over calcium hydride for 24 h, and distilled under reduced pressure before use. Toluene, used as the solvent, was purified by refluxing over calcium hydride for 24 h, followed by fractional distillation. Methylaluminoxane (MAO) was prepared from $AlMe_3$ (TMA) and $CuSO_4 \cdot 5H_2O$ according to the literature [13] and reserved as stock solution in toluene, 1.04 mmol ml^{-1}. The TMA and $CuSO_4 \cdot 5H_2O$ were commercially obtained

* Corresponding author.

0032-3861/98/$ - see front matter
PII: S0032-3861(98)00372-3

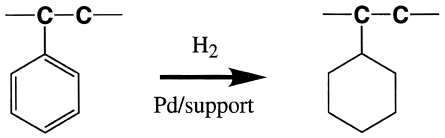

Fig. 1. Reaction schematic of hydrogenation chemistry.

from Tosoh Akzo Chemical Co. and Nacalai Tesque Co., respectively, and were used without further purification. η-$C_5(CH_3)_5TiCl_3$ was synthesized according to the literature [14].

Polymerization of styrene was carried out at 343 K in a 100 ml glass reactor equipped with a magnetic stirrer under nitrogen atmosphere, using toluene as the solvent. The polymerization was quenched by adding acidic methanol. The polymer produced was separated by filtration, dried under reduced pressure at 333 K and by exhaustive extraction with boiling methyl ethyl ketone in a soxhlet extractor. The resulting samples were then dissolved in boiling xylene to remove the catalyst. The filtrates were reprecipitated in methanol, and the powdery samples thus obtained were dried in a vacuum oven at 393 K for 40 h. Glassy films of sPS were prepared by compression moulding as follows: the purified sPS sample was pressed at 563 K under 10 MPa for 8 min and immediately quenched into an ice–water bath.

The hydrogenation reaction of syndiotactic polystyrene (sPS) was conducted under 12 MPa at 463 K in methylcyclohexane using a Pd(5 wt%)–$BaSO_4$ catalyst (0.1 g catalyst/g polymer). The catalyst was commercially obtained from Aldrich Chemical Co. and used without further purification. The methylcyclohexane (Nacalai Tesque Co.) was distilled over calcium hydride before use. The degree of hydrogenation was controlled by changing the reaction time from 6 to 72 h. Fig. 1 shows a reaction schematic of the hydrogenation chemistry. The nomenclature used in this paper is as follows: e.g., HsPS61 denotes a hydrogenated syndiotactic polystyrene with a hydrogenation degree of 61 wt%. The resulting materials were dissolved in boiling xylene up to 1 wt% and successively filtered to remove the catalyst. The filtrates were reprecipitated in methanol containing a small amount of an antioxidant, and the samples were dried in a vacuum oven at 393 K for 40 h. The powdery samples thus obtained were pressed at 563 K under 10 MPa for 8 min and immediately quenched into an ice–water bath (quenched films). For comparison, slowly cooled films were also prepared by cooling the samples down (at about $-2\ K\ min^{-1}$) to the glass transition temperature.

2.2. Measurements

The molecular weight and molar mass distribution (MMD) of hydrogenated syndiotactic polystyrenes (HsPS) were determined by a high temperature gel permeation chromatography instrument (Senshu Scientific SSC-7100) using *o*-dichlorobenzene as the solvent at 403 K (see Table 1).

Table 1
Characteristics of samples

Sample	Reaction time (h)	Degree of hydrogenation[a]		$\bar{M}_w \times 10^{-5}$	$\bar{M}_w/\bar{M}_n$
		mol%	wt%		
sPS	0	0	0	5.2	2.6
HsPS5	6	5	5	5.1	2.6
HsPS19	12	18	19	4.8	3.2
HsPS23	15	22	23	4.6	3.2
HsPS42	22	41	42	5.0	2.9
HsPS61	40	60	61	5.0	3.2
HsPS73	48	72	73	4.9	3.1
HsPS100	72	97	97	4.4	3.7

[a]Estimated by ^1H NMR.

The degree of hydrogenation was determined by ^1H nuclear magnetic resonance (NMR). The 300 MHz ^1H NMR spectra were recorded on a Varian Gemini 300 spectrometer at 313 K on 10% (w/v) solutions in $CDCl_3$. The stereoregularity of samples was determined by ^{13}C NMR at 373 K on 10% (w/v) solutions in 1,2,4-trichlorobenzene/C_6D_6.

Differential scanning calorimetry (DSC) measurements were made with a Mettler DSC 820. The samples, weighing about 10 mg, were sealed in aluminium pans. Measurement of the samples was carried out at a heating rate of $20\ K\ min^{-1}$.

Small angle light scattering (SALS) measurement was carried out with a commercial light-scattering photometer (IST Planning SALS-100S) using a He–Ne laser. The detector used was a photomultiplier that can rotate horizontally around a sample to scan scattering angles from 0° to 20°. The samples used for the SALS measurements were about 50 μm thick.

Dynamic mechanical properties were investigated using a dynamic mechanical analyser (Rheology Co. Ltd, DVE V-4) on sample specimens of the following dimensions: length 15 mm, width 3 mm, thickness about 300 μm. The temperature dependences of the dynamic tensile moduli, storage tensile modulus E' and loss modulus E'' were measured between 113 and 543 K at a constant frequency of 50 Hz and a heating rate of $2\ K\ min^{-1}$.

3. Results and discussion

3.1. Sample characterization

Fourier transformation infrared (FTIR) spectra were examined at a resolution of $2\ cm^{-1}$ with a JASCO FT-IR 500 spectrometer. As shown in Fig. 2, the intensity of the 890 cm^{-1} band assigned to the cyclohexyl ring [5] increases with increasing hydrogenation degree for both Q- and SC-films. In the case of Q-films, the loci of the 906 cm^{-1} band assigned to aromatic ring CH out-of-plane deformation remain the same with the hydrogenation degree, suggesting

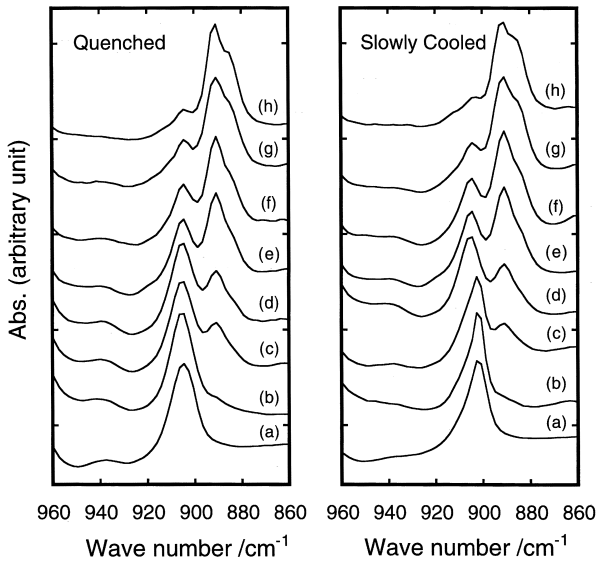

Fig. 2. Infrared spectra of the HsPS films: (a) sPS; (b) HsPS5; (c) HsPS19; (d) HsPS23; (e) HsPS42; (f) HsPS61; (g) HsPS73; (h) HsPS100.

that these Q-films are in the amorphous state at room temperature, as is also seen in the Q-films of HaPS [8]. On the other hand, in the spectra of SC-films for sPS, HsPS5 and HsPS19, the 906 cm^{-1} band shifts to lower frequencies due to the increase of the crystallized sPS sequence [15]. The band does not shift any further even when the hydrogenation degree increases from 23% to 100%, which indicates that these samples do not have crystallizable sPS sequences.

The molecular aggregation state of HsPS(Q) films was examined using a small-angle light scattering (SALS) technique. Our previous results on partially hydrogenated atactic polystyrene (HaPS) suggested the formation of a phase-separated morphology; i.e., aPS domains are dispersed within the HaPS matrix. As shown in Fig. 3, the Debye–Bueche model is found to be applicable only for partially hydrogenated films such as HsPS42(Q), HsPS61(Q), and HsPS73(Q), suggesting that these films form multiphase morphology as is also seen in HaPS films. The correlation lengths, corresponding to the average distance between

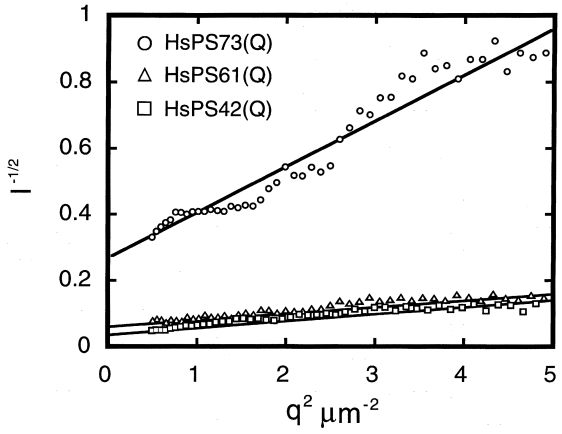

Fig. 3. Debye–Bueche plots for the HsPS films.

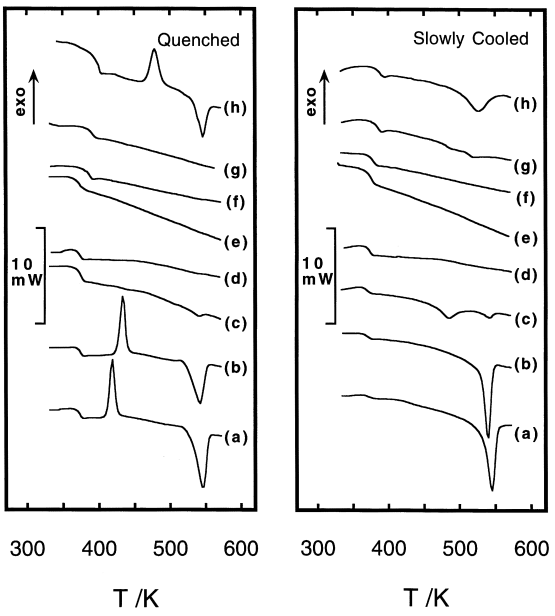

Fig. 4. DSC curves for the HsPS films: (a) sPS; (b) HsPS5; (c) HsPS19; (d) HsPS23; (e) HsPS42; (f) HsPS61; (g) HsPS73; (h) HsPS100. Heating rate: 20 K min^{-1}.

neighbouring domains [16], can be derived from the ratio of slope to intercept. The resulting correlation length was 0.38 μm for HsPS42(Q), 0.29 μm for HsPS61(Q) and 0.78 μm for HsPS73(Q).

The DSC curves of the HsPS(Q) and HsPS(SC) films are shown in Fig. 4. The sPS(Q) displays a crystallization (exothermic) peak T_c at 418 K as well as a melting (endothermic) peak T_m at 546 K. The exothermic and endothermic peaks of the Q-films disappeared with an increase in the hydrogenation degree. It is considered likely that the bulkiness effect of the cyclohexane group prevents the sPS sequence from crystallizing. However, the completely HsPS100(Q) film showed a crystallization temperature of 479 K and a melting temperature of 546 K. Wide angle X-ray analysis of HsPS100 also exhibited a crystalline pattern. In the case of SC-films, on the other hand, the HsPS with lower hydrogenation exhibited only a melting temperature at 540 K, which is the same as the T_m of sPS films, whereas HsPS films with higher hydrogenation than 73% exhibited a T_m at 529 K. Moreover, SC-films with hydrogenation in the range from 23% to 61% were found to be uncrystallizable. The T_m and the heat of fusion ΔH_f for HsPS(SC) films are summarized in Table 2.

3.2. Effect of crystallinity on glass transition

Figs 5 and 6 show the temperature dependence of storage moduli (E') and loss moduli (E'') for quenched and slow-cooled films of various HsPS samples, respectively, in the temperature range from 350 K to 560 K. There is a sharp peak between 370 K and 430 K ascribed to glass transition T_g for both films, as observed in the DSC curves (Fig. 4).

Table 2
Thermal properties of HsPS(SC) films

Sample	T_m (K)[a]	ΔH_f (J g^{-1})[b]
sPS	545	34.5
HsPS5	540	30.7
HsPS19	486, 538	13.3
HsPS23	n.d.[c]	n.d.
HsPS42	n.d.	n.d.
HsPS61	n.d.	n.d.
HsPS73	519	7.8
HsPS100	529	22.3

[a]Melting temperature.
[b]Heat of fusion.
[c]Not detected.

The E' and E'' of the sPS(Q), HsPS5(Q) and HsPS100(Q) films, which are crystallizable polymers, recover at around T_c, suggesting that the recovery of moduli must be associated with the crystallization process [17].

Compared with the T_g peak for Q films, the corresponding T_g peak for the SC films is much broader. Fig. 7 compares the plot of E'' versus $1/T$ around T_g for sPS(SC) and HsPS100(SC) films. As seen in the figure, the subtraction of the T_g peak (designated as T_g(Q)) of the Q films from the T_g dispersion of the SC films gives an additional T_g peak (designated as T_g(SC)) in the high temperature region. The T_g(SC) presumably arises from the relaxation process of the amorphous component under restraint by its crystalline parts [18]. As seen in Fig. 8, the semilogarithmic plot of the frequency thus obtained against $1/T$ yields the apparent activation energy ΔH, giving 742 and 571 kJ mol^{-1}, respectively, for the T_g(SC) processes of sPS and HsPS100, and 478 and 465 kJ mol^{-1}, respectively, for the T_g(Q) of sPS and HsPS100. The ΔH for T_g(SC) is found to be considerably larger than the ΔH value for T_g(Q). This will be because the molecular mobility of the amorphous component of SC films is restrained by the crystalline component.

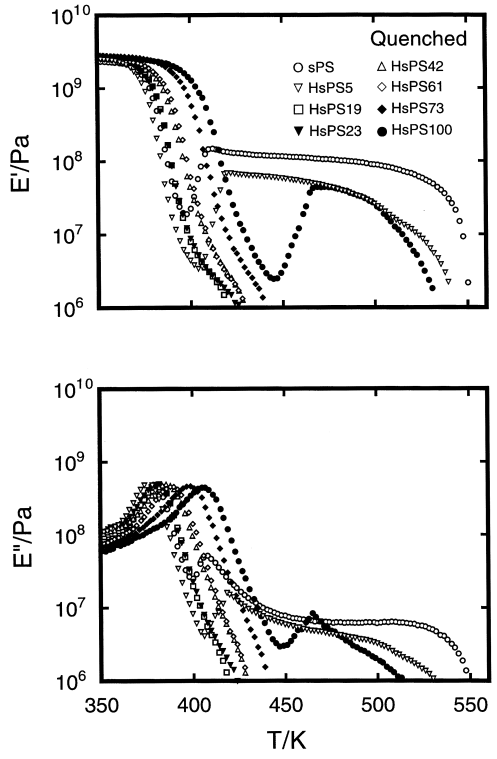

Fig. 5. Temperature dependence of mechanical storage modulus (E') and loss modulus (E'') in the region of primary dispersion for all the quenched films.

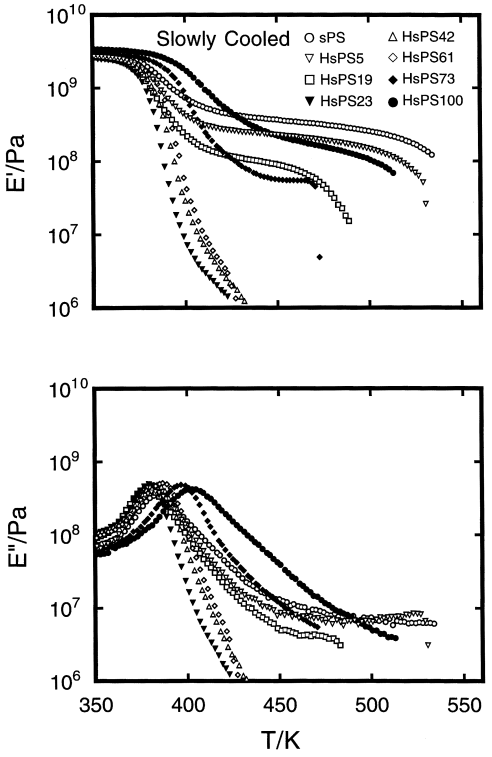

Fig. 6. Temperature dependence of mechanical storage modulus (E') and loss modulus (E'') in the region of primary dispersion for all the slowly cooled films.

In order to characterize the overlapping behaviour of the primary dispersion in the crystallized HsPS samples, we examined the half-width of the dispersion, determined by the width at half maximum in the plot of E'' versus $1/T$. Fig. 9 shows the plot of $\Delta_{1/2(SC)} - \Delta_{1/2(Q)}$ (the subtraction of $\Delta_{1/2}$ for HsPS(Q) from $\Delta_{1/2}$ for HsPS(SC)) versus the degree of hydrogenation.

The value of $\Delta_{1/2(SC)} - \Delta_{1/2(Q)}$ attained a minimum at around medium degree of hydrogenation, as seen in Fig. 9. The value of $\Delta_{1/2(SC)} - \Delta_{1/2(Q)}$ is apparently dependent on the value of ΔH_f, suggesting that $\Delta_{1/2(SC)} - \Delta_{1/2(Q)}$ is closely related to the degree of crystallinity for the HsPS samples.

3.3. Motion of cyclohexyl group

In our previous paper [8], we reported that HaPS showed two relaxation dispersions, designated β and γ, between 110

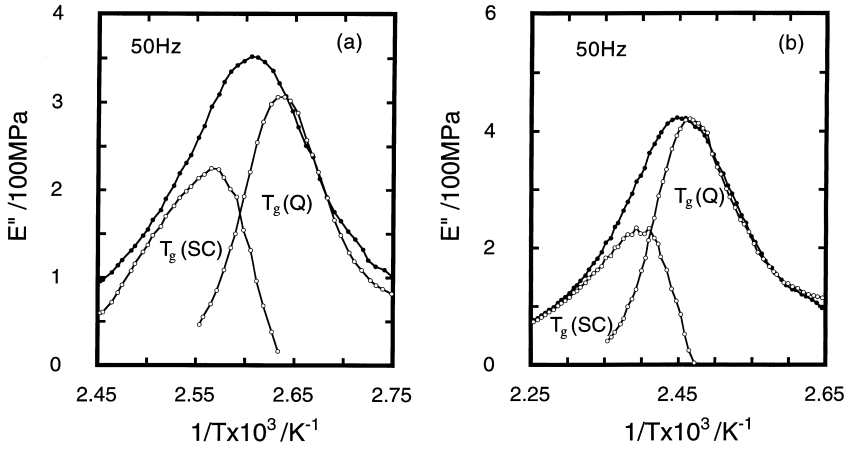

Fig. 7. Plot of E'' versus the inverse of temperature for the crystalline polymers in the region of primary dispersion: (a) sPS(SC); (b) HsPS100(SC). T_g(Q) relates to purely amorphous components; T_g(SC) relates to amorphous components under restraint by crystallites.

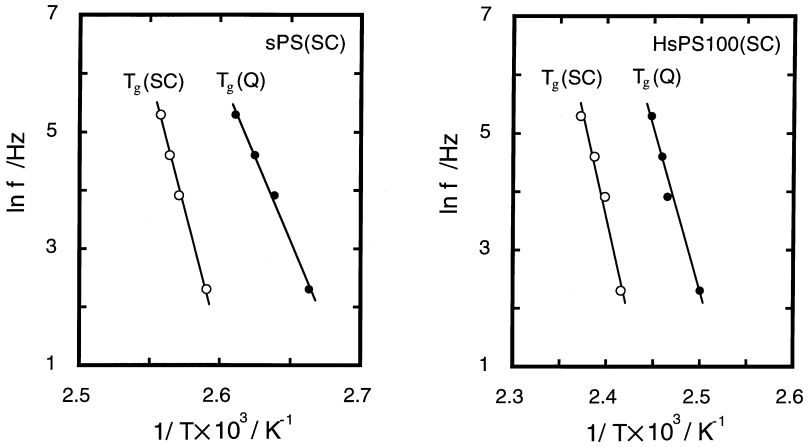

Fig. 8. Logarithm of frequency plotted against inverse of temperature for crystalline polymers: (a) sPS(SC); (b) HsPS100(SC).

and 250 K. The β dispersion, at higher temperatures, is associated with chair–chair flip motions of the cyclohexyl group, and the lower-temperature relaxation peak (γ) involves various specific vibrational modes including oscillatory rotation of the cyclohexyl group around a bond between the substituent and the backbone chain.

The temperature dependences of loss tangent ($\tan\delta = E''/E'$) for the various HsPS(Q) films between 110 and 250 K are shown in Fig. 10. With increasing hydrogenation degree, both β and γ peaks undergo increases, but the loci of both peaks do not change. The dispersions are scarcely evident for sPS. This behaviour of the dynamic mechanical spectra is similar to that of hydrogenated aPS.

Fig. 11 shows the behaviour of $\tan\delta$ for HsPS(SC) films. The overall strength of the β and γ peaks for HsPS100(SC) is lower than that for HsPS100(Q), suggesting that the molecular motions of the cyclohexyl group in the crystalline part are sterically hindered. As seen in the figure, the HsPS5(SC) and HsPS19(SC) films having sPS crystals significantly promote the γ peaks and suppress the β peaks. Although the

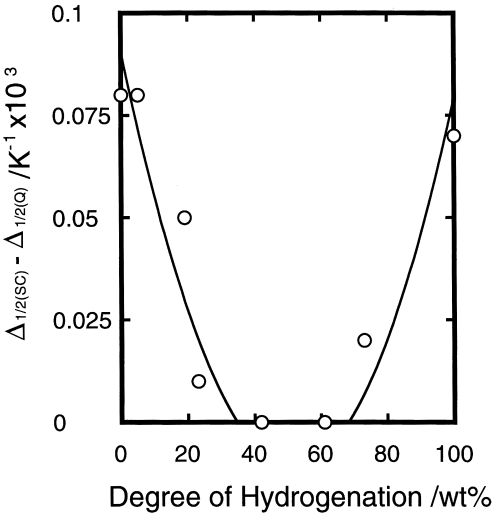

Fig. 9. Dependence of $\Delta_{1/2(SC)} - \Delta_{1/2(Q)}$ on the degree of hydrogenation. $\Delta_{1/2(SC)}$ and $\Delta_{1/2(Q)}$ are the widths at half maximum in the plots of E'' against $1/T$ for HsPS(SC) and HsPS(Q) respectively.

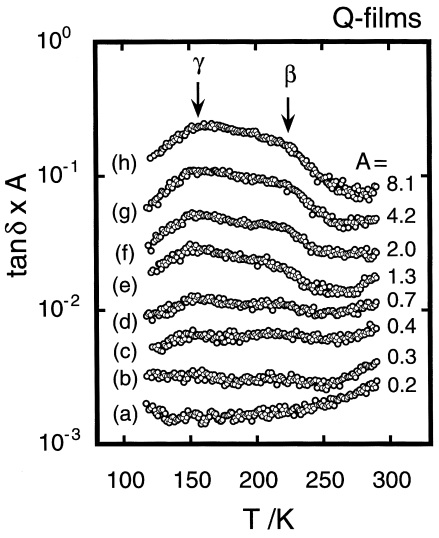

Fig. 10. Plots of loss tangent (tan δ) for HsPS(Q) in the region of secondary dispersion: (a) sPS; (b) HsPS5; (c) HsPS19; (d) HsPS23; (e) HsPS42; (f) HsPS61; (g) HsPS73; (h) HsPS100.

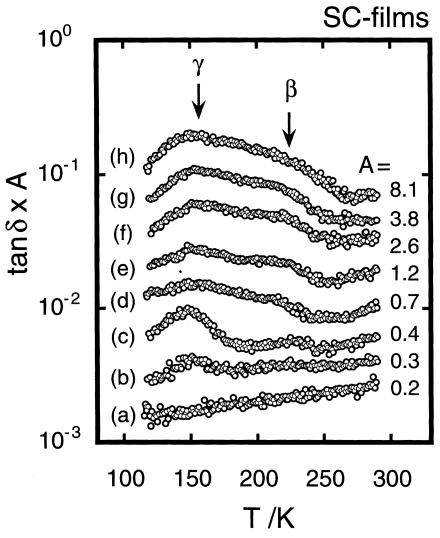

Fig. 11. Plots of loss tangent (tan δ) for HsPS(SC) cooled films in the region of secondary dispersion: (a) sPS; (b) HsPS5; (c) HsPS19; (d) HsPS23; (e) HsPS42; (f) HsPS61; (g) HsPS73; (h) HsPS100.

origin of such behaviour has not yet been clarified, large-scale molecular motion such as chair–chair flip may be hindered by the existence of the crystallized sequence of sPS.

4. Conclusions

In the present study, we have examined the effects of cyclohexyl content on the dynamic mechanical relaxation processes for hydrogenated syndiotactic polystyrene (HsPS) having various degrees of hydrogenation. In the case of crystalline HsPS samples, the primary dispersion was much broader than that of glassy samples. The broadness of dispersion will be due to the overlapping of two glass relaxation processes arising from one purely amorphous component and the other amorphous component which is under restraint due to the proximity of crystallites.

Moreover, it was found that the HsPS samples show the two relaxation processes ascribed to the cyclohexyl side group in the range from 110 to 250 K, as was also observed in completely hydrogenated atactic PS. The dynamic mechanical spectra suggest that the mobility of the cyclohexyl group of crystallized completely hydrogenated sPS (HsPS100) becomes significantly lower than that of glassy HsPS100.

References

[1] Mays J, Hadiichristidis N, Fetters LJ. Macromolecules 1984;17:2723.
[2] Bates FS, Rosedale JH, Bair HE, Russell TP. Macromolecules 1989;22:2557.
[3] Krishnamoorti R, Graessley WW, Balsara NP, Lohse DJ. Macromolecules 1994;27:3073.
[4] Frosini V, Magagnini P, Butta E, Baccaredda M. Kolloid-Z Z Polym 1966;213:115.
[5] Abe A, Hama T. Polym Lett 1969;7:427.
[6] Gehlsen MD, Bates FS. Macromolecules 1993;26:4122.
[7] Gehlsen MD, Peter A, Weimann FS, Bates FS, Harville S, Mays JW, Wignall GD. J Polym Sci, Part B, Polym Phys 1995;33:1527.
[8] Nakatani H, Nitta K, Soga K. Polymer, in press.
[9] Ishihara N, Seimiya T, Kuramoto M, Uoi M. Macromolecules 1986;19:2464.
[10] Kobayashi M, Nakaoki T, Ishihara N. Macromolecules 1989;22:4377.
[11] Guerra G, Vitagliano VM, De Rosa C, Petraccone V, Corradini P. Macromolecules 1990;23:1539.
[12] Nakatani H, Nitta K, Uozumi T, Soga K. Polymer Commun, in press.
[13] Sinn H, Kaminsky W, Vollmer HJ, Woldt R. Angew Chem, Int Ed Engl 1980;19:390.
[14] Yamamoto H, Yasuda H, Tasumi K, Lee K, Nakamura A. Organometallics 1995;8:105.
[15] Auriemma F, Petraccone V, Dal Poggetto F, De Rosa C, Guerra G, Manfredi C, Corradini P. Macromolecules 1993;26:3772.
[16] Khabatta FB, Warner F, Russell T, Stein RS. J Polym Sci, Polym Phys Ed 1976;14:1391.
[17] Nakatani H, Nitta K, Soga K. Rep Prog Polym Phys Jpn 1996;39:449.
[18] Boyer RF. J Polym Sci, Symp 1975;50:189.